Multicomponent blood analysis by near-infrared Raman spectroscopy

Andrew J. Berger, Tae-Woong Koo, Irving Itzkan, Gary Horowitz, and Michael S. Feld

We demonstrate the use of Raman spectroscopy to measure the concentration of many important constituents (analytes) in serum and whole blood samples at physiological concentration *in vitro* across a multipatient data set. A near-infrared (830-nm) diode laser generates Raman spectra that contain superpositions of Raman signals from different analytes. Calibrations for glucose, cholesterol, urea, and other analytes are developed by use of partial least-squares cross validation. We predict six analytes in serum with significant accuracy in a 66-patient data set, using 60-s spectra. The calibrations are shown to be fairly robust against system drift over the span of seven weeks. In whole blood, a preliminary analysis yields accurate predictions of some of the same analytes and also hematocrit. The results hold promise for potential medical applications. © 1999 Optical Society of America

OCIS codes: 170.1470, 170.5660.

1. Introduction

Many researchers have investigated methods of measuring blood constituents (analytes) optically. These approaches include absorption (both mid-infrared[1–7] and near-infrared[8–17]), polarization,[18–20] elastic scattering,[21–23] photoacoustic,[24] and various types of Raman (spontaneous Stokes[25–30] and anti-Stokes,[31] and stimulated Stokes[32,33]). In many cases, the underlying goal is to develop a noninvasive technique for monitoring one or more analytes; in other situations, simpler or more accurate off-line, *in vitro* measurements are sought. Interest in this field is strong, particularly within the community of diabetic patients for whom glucose monitoring is a critical application.

In previous research we used near-infrared Raman spectroscopy and multivariate calibration methods to extract analyte concentrations from aqueous samples[34] and single-donor doped whole blood,[35] in both cases at high concentrations. Here we extend the Raman approach to demonstrate *in vitro* measurement of analytes in serum and whole blood samples from a large (69 samples), multipatient data base. The samples are obtained directly from a local hospital and contain analytes at physiological concentrations. Using integration times of 1 min or less, we predict multiple analytes' concentrations in the serum samples with significant accuracy. A preliminary analysis of the whole blood data, without correction for the turbidity of the samples, shows that analyte detection is possible even in the absence of such correction. The results indicate the potential value of Raman spectroscopy for applications in blood analyte monitoring.

2. Experimental Methods

A. Blood Samples

Blood samples were obtained from 69 patients at Beth Israel Deaconess Medical Center. Part of each sample was allowed to clot and then centrifuged, thereby removing all cellular components and clotting proteins. Each of the resulting serum samples was then analyzed on the hospital's commercial instrument to yield concentrations of a set of analytical quantities, and the remainder was refrigerated at 4 °C. Another portion of the blood was mixed with an anticlotting agent (EDTA) and analyzed for hematocrit (red blood cell volume fraction). As with serum, the remainder of the whole blood sample was refrigerated at 4 °C as soon as possible; however, hospital protocol did not permit good control over this

When this research was performed, A. J. Berger, T.-W. Koo, I. Itzkan, and M. S. Feld were all with the G. R. Harrison Spectroscopy Laboratory, Massachusetts Institute of Technology, Cambridge, Massachusetts 02139. A. J. Berger (ajberger@bli.edu) is now with Beckman Laser Institute, 1002 Health Sciences Road, Irvine, California 92612. G. Horowitz is with Beth Israel Deaconess Medical Center, Boston, Massachusetts 02215.

Received 29 July 1998; revised manuscript received 8 February 1999.

0003-6935/99/132916-11$15.00/0

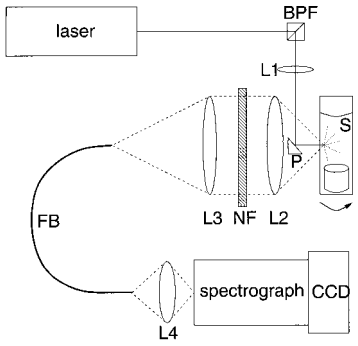

Fig. 1. Experimental setup for acquisition of Raman spectra from blood samples: BPF, bandpass filter; P, prism; S, blood sample; L1–L4, lenses; NF, notch filter; FB, fiber bundle. See text for details.

step, so a variable delay of as much as 3 h of the samples' sitting at room temperature was introduced. During this time, the glucose level could decay significantly, and other analyte levels might also change.[36,37] In an effort to obtain a more relevant glucose reading, a portion of each refrigerated whole blood sample was removed, centrifuged, and analyzed for plasma glucose concentration on the morning of the day on which Raman spectra were acquired. It was this reading that was used as the reference concentration. From each of 69 patients, therefore, we obtained two samples (serum and whole blood) and three printouts listing serum analyte levels, the whole blood hematocrit, and the corrected plasma glucose level for the whole blood sample.

Samples were obtained over a span of seven weeks. Each week, samples from 8 to 11 patients were received, for a total of 69 samples each of serum and whole blood. To perform the spectral measurements, we transported the refrigerated samples from the Beth Israel Deaconess Medical Center to the MIT laboratory, which was approximately 15 min away by car.

All the blood samples were drawn from patients for other purposes. Our assisting technicians attempted to find some samples with extreme glucose concentrations to represent the range of diabetic patients' glucose levels; no other selection criterion was used in choosing samples. The vast majority of the samples came from relatively stable patients with mostly normal blood analyte levels.

B. Raman Spectroscopy System

A schematic of the Raman spectroscopy system is shown in Fig. 1. Near-infrared light at 830 nm is supplied by a diode laser (SDL) and filtered by a holographic grating (Kaiser). The laser beam is directed onto the blood samples via a prism mounted in the umbra of a Cassegrain microscope objective (Ealing); this arrangement makes the delivery and collection optics coaxial. Light collected by the microscope objective is notch filtered, transformed by a fiber optic bundle into a line, and imaged onto the slit of an $f/1.8$ spectrograph (Kaiser). The spectrograph disperses the image of the slit horizontally across a two-dimensional CCD array detector, 1152 pixels wide by 770 pixels high. Spectra were created by binning of the CCD output into tall superpixels, resulting in an 1152-element spectrum. Overlapped spectra of 20 representative serum samples, measured from two different weeks, are shown in Fig. 2(a); 20 spectra of whole blood samples appear in Fig. 2(b). The spectral resolution of the data is 6 cm^{-1}.

The total spectral acquisition time per sample was 5 min (an arbitrary time chosen for the convenience of running multiple samples in an afternoon), divided into 30 frames of 10 s each that were first processed to remove spurious cosmic ray signals (with a frame-by-frame comparison to identify outlying spectral data points) and then coadded. Methanol spectra were measured several times each day to provide corrections for laser intensity fluctuations. Spectra corresponding to a range of integration times from 10 s to 5 min could thus be created for a single sample. We exploited this degree of freedom during the data analysis, using the full 5 min per spectrum when

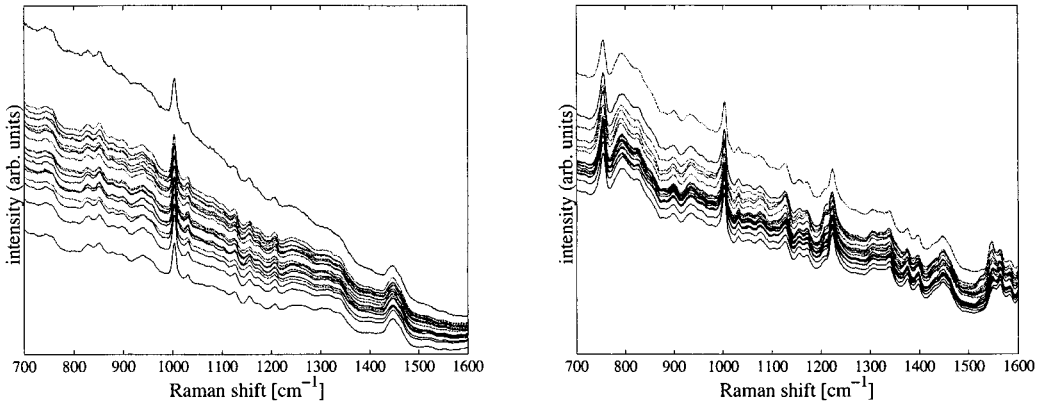

Fig. 2. Twenty spectra from each of the two data sets, demonstrating the typical spread in the data: (a) serum, (b) whole blood.

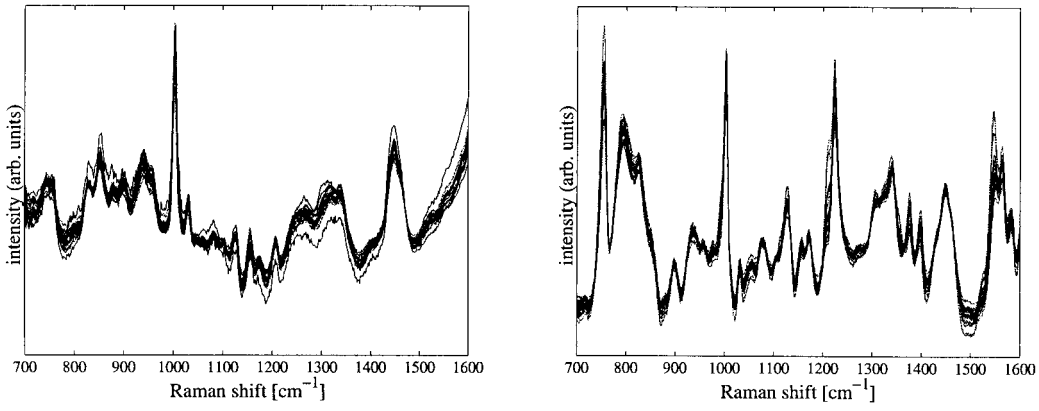

Fig. 3. Same data as in Fig. 2 after linear baseline subtraction, which removes the gross fluctuations, creating better overlap and emphasizing Raman peaks: (a) serum, (b) whole blood.

building the concentration prediction algorithms but using shorter amounts of time when submitting spectra for concentration prediction, for reasons explained below.

To minimize heating artifacts caused by the high laser intensity (250 mW focused into a spot approximately 50 μm in diameter), we stirred the blood samples continuously, using a magnetically driven cylindrical pellet. As shown in Fig. 1, the pellet sat at the base of the sample cuvette, below the laser interaction region. Using this method, we reduced the heating effects sufficiently to obtain the results described. However, small time-dependent drifts in the spectra were still observed, and the samples in the cuvettes felt warm to the touch after 8 min of laser exposure (including the dead time from 30 CCD readouts), so heating was not completely eliminated. Temperature was not explicitly measured in this initial investigation; in a future experiment we intend to monitor and control it and determine its significance, if any.

C. Spectral Background Removal

As Fig. 2 shows, measured blood spectra consist of multiple sharp Raman peaks, 10 to 50 cm^{-1} in width, riding atop a background that, while it is fairly flat, varies considerably from sample to sample. These fluctuations do not correlate with any analyte's concentration. However, spectra from the same week tend to bunch together in the plot (not discernible in the figure), suggesting that the background is influenced by changes in system alignment. The background was removed mathematically by subtraction of a sloped straight line from each spectrum by least-squares fitting; this procedure minimally affected the shape of the Raman peaks. In the resulting background-subtracted spectra of serum and whole blood, shown in Fig. 3, the spectra overlap much more nearly completely than before.

The strong peak of phenylalanine near 1000 cm^{-1} was used as an internal wave-number standard. In the spectra from weeks 5–7 this peak was observed to have shifted by one CCD pixel element relative to those from the first four weeks. Therefore, before data analysis, the spectra from these later weeks were mathematically shifted to align the peaks with those of the earlier weeks.

D. Multivariate Data Analysis

If the blood Raman spectra are linear superpositions of the constituent analytes' spectra, with each spectral contribution proportional to that analyte's concentration,[25,27,34] one can extract concentrations from the spectral data by using linear multivariate calibration, with the best method of extraction depending on the breadth of calibration data available. The method of partial least squares[38–40] (PLS) was chosen because it is designed to predict the concentration of an analyte even when other analytes are present and varying in unknown ways, as is the case with blood samples. Like all other linear methods, PLS predicts a concentration by forming a weighted linear combination of the measured spectral intensities. The weighting coefficients can themselves be plotted as a spectrum that is sometimes called the regression vector, or b-vector; various formulas exist for computing the b-vector from a PLS calibration.[38,41] In a system that contains N constituents, each analtye's spectrum can be regarded as the sum of two line shapes, one of which can be modeled completely by the other $N - 1$ analytes' spectra and one of which is orthogonal to their spectra. The second of these two line shapes is the b vector. As such, the b-vector represents that which is unique about an analyte's spectral signature. It is therefore a useful diagnostic tool for interpreting a PLS calibration. Prominent features of the b-vector indicate spectral regions that contain information about the concentration of the target analyte. Different b-vectors can extract different analytes' concentrations from the same spectrum. Another source of valuable qualitative information is provided by the sets of basis spectra

Table 1. PLS Prediction Results for Serum Data Set

Analyte	Reference Error	RMSEP	r^2	Integration Time (s)	Spectral Range (cm^{-1})	PLS Model Rank
Glucose	3 mg/dL	26 mg/dL	0.83	60	720–1602	11
Cholesterol	4 mg/dL	12 mg/dL	0.83	60	565–1746	9
Triglyceride	3 mg/dL	29 mg/dL	0.88	60	565–1746	10
BUN (urea)	0.9 mg/dL	3.8 mg/dL	0.74	60	720–1602	10
Total protein	0.1 g/dL	0.19 g/dL	0.77	10	565–1746	10
Albumin	0.09 g/dL	0.12 g/dL	0.86	10	720–1602	4

derived by PLS to model the sample spectra. These line shapes are called weight and loading vectors, and the weight vectors in particular often contain spectral features that are noticeably similar to those of a known constituent.[38] Unlike the *b*-vector, which reflects the overall calibration algorithm, no single weight vector is guaranteed to contain recognizable spectral features of the target analyte; however, inasmuch as the *b*-vector inherently contains a mixture of the target analyte's spectrum and other analyte's spectra,[41] peaks from the target analyte can appear more clearly in weight vectors, without so much interference. The signal-to-noise ratio (SNR) of peaks in the first few weight vectors is also usually better than in the *b*-vector, which is a weighted sum of many weight and loading vectors, some of which have much worse SNR's.

Background-subtracted spectra of serum and whole blood were provided, along with the measured reference concentrations of various analytes, to the PLS algorithm. The spectra were binned over five pixels to create a pixel spacing of $\sim 8\ cm^{-1}$ (the wavenumber dispersion of the spectrograph is not constant across the spectrum); other bin sizes were tested and led to prediction accuracies similar to those reported below. The portions of the spectra below $565\ cm^{-1}$ and above $1746\ cm^{-1}$ were discarded, the former because of the cutoff limit of the notch filter to remove the 830-nm laser line, the latter because of the falloff in sensitivity of the CCD detector. The PLS algorithm mean-centered the spectra and the concentrations as its first step.[38] Using PLS, we constructed *b*-vectors to predict the concentration of glucose, urea, cholesterol, triglyceride, total protein, albumin, and hematocrit in both serum and whole blood. We assessed the accuracy of the PLS predictions by computing the root-mean-squared error of prediction (RMSEP) for each analyte in each of the two blood media. Once a calibration was established, the prediction of a sample's concentration took less than a second.

To test the robustness of the PLS modeling, a leave-one-week-out cross validation was used. All calculations were performed in MATLAB with in-house routines. PLS *b*-vectors were developed with spectra from six of the weeks and then applied to the spectra from the seventh week to generate concentration predictions, with each week rotated out in turn until all samples were predicted. By cycling out an entire week's samples at once, we prevented any information about their spectral backgrounds from influencing the *b*-vector. We chose this approach specifically to test for robustness against system fluctuations from week to week; leave-one-sample-out cross validations can exhibit spurious ability to correct for such fluctuations.[15,42] Although our observation was that our system background varied randomly from one week's alignment to the next, we also performed supplementary leave-half-out validations in which the first four weeks' data were used to predict concentrations in the last three weeks' and vice versa. These extra validations, in which the calibration and prediction sets were formed from nonoverlapping time periods, tested for robustness against time-dependent system drift on the scale of weeks.

In each case, the full 5 min of spectral data for the six calibration weeks were used but the time for the predicted week was systematically reduced until we began to sacrifice prediction accuracy in the cross validation. Different time limits were reached for different analytes, as discussed below. The different treatment of the integration times for calibration and prediction reflects the practical constraints on blood analyzers: Whereas an instrument's calibration data can be collected over relatively long times, in most instances the clinical performance must be as rapid as possible.

3. Results and Discussion

A. Serum

1. *Prediction Accuracy*

Table 1 lists, for the serum data set, the parameters of the PLS cross validation and the resulting RMSEP values for each of six analytes: glucose, total cholesterol, triglyceride, urea (reported in clinicians' units of blood urea nitrogen, or BUN), total protein, and albumin. Although similar PLS analyses were attempted, no prediction accuracy was observed for the other analytes measured by the analyzer (creatinine, sodium, potassium, chloride, carbon dioxide, alanine transaminase, aspartate transaminase, lactate dehydrogenase, creatine kinase, alkaline phosphatase, total bilirubin, direct bilirubin, calcium, phosphate, magnesium, uric acid, and iron). Some of these additional analytes are monatomic and are not expected

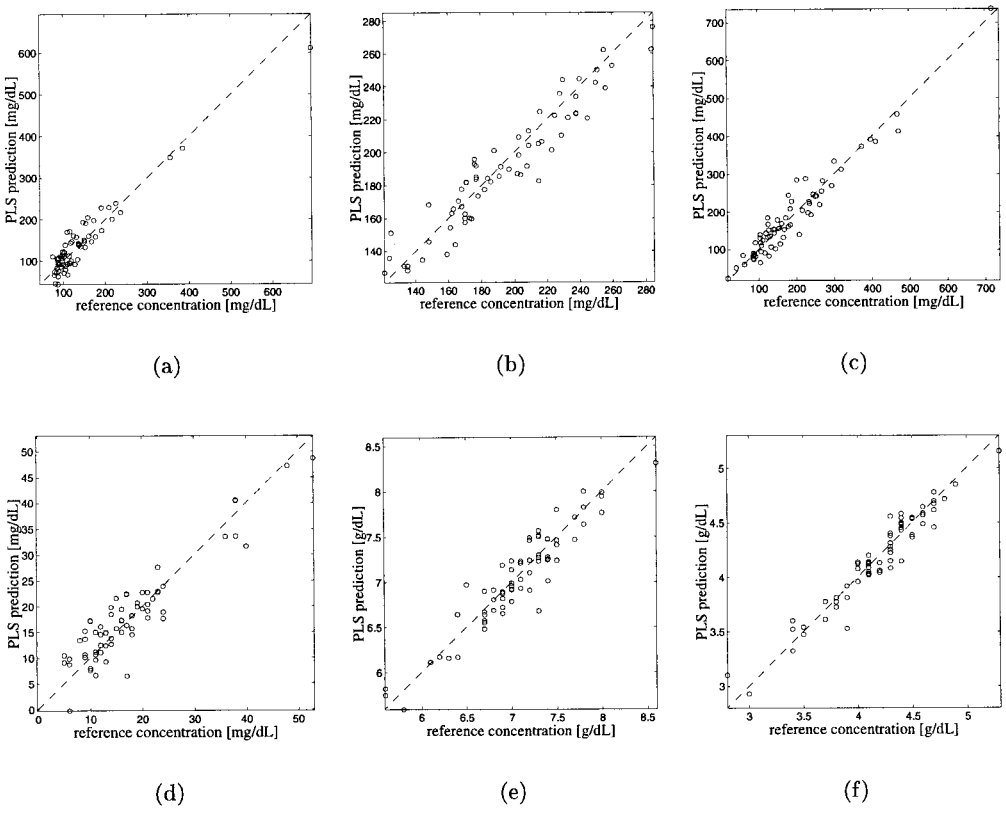

Fig. 4. PLS predictions of analyte concentrations in serum data: (a) glucose, (b) cholesterol, (c) triglyceride, (d) urea (BUN), (e) total protein, (f) albumin.

to generate Raman scattering signals; the remainder generate sufficiently low signals, because of low concentration or low Raman cross section, that they cannot be detected over the spectral noise in the acquired data, although longer integration times might have yielded different results. The corresponding plots of predicted versus reference concentrations for the six analytes appear in Fig. 4. All six plots show a visible correlation between the predicted and the reference concentrations, with r^2 values of 0.74 or higher. Of the 69 samples, 2 were contaminated by handling errors and 1 yielded a spectrum with twice the background of any other as the result of an obvious heating residue formed on the cuvette's inner surface during data acquisition; all the remaining 66 were included in the cross validation.

Spectral bin size, spectral range, and model rank (number of iterations of the PLS modeling loop) are all free parameters in a PLS model. Excessive variation of their values in a cross-validation study can lead to spurious minimization of the RMSEP. The spectral bin size and range were chosen based on physical considerations (the natural linewidth of typical biological Raman bands and the detection window of our spectrometer–CCD system, respectively). All analytes reported here were predicted accurately by use of these parameters, with RMSEP values that were insensitive to small changes in the spectral range end points. A second, smaller spectral range (720–1602 cm^{-1}) was also explored and yielded slightly better results for three of the six analytes. Model rank was chosen to minimize the RMSEP, but the dependence on rank was always weak in the vicinity of the minimum, as expected for robust predictions.[38,39]

All the analytes were predicted just as accurately with 60-s spectra as with the full 5-min spectra. When the time was reduced still further, predictions of four of the analytes began to degrade, implying that the shrinking spectral SNR was now the limiting source of prediction error.[41] However, albumin and total protein accuracy remained unchanged, even at 10 s. Two observations help to explain this result. First, proteins are the dominant constituents of serum, and many of the dominant peaks in the serum Raman spectra can be assigned to proteins,[43,44] so the spectral SNR for proteins is higher than for other analytes. In addition, note from Table 1 that the hospital reference analyzer's precision, determined by the running of quality control standards, is nearly the same as the RMSEP for these two analytes. Under such conditions, the analyzer's own uncertainty becomes a limiting source of prediction error. In the case of albumin, it is even likely that the PLS calibration would prove to be more accurate than the hospital analyzer if it were tested against a more-accurate standard.[45] Taken together, these observations suggest an explanation for the stability of the protein predictions: The spectral SNR may be sufficiently high that it does not affect the prediction

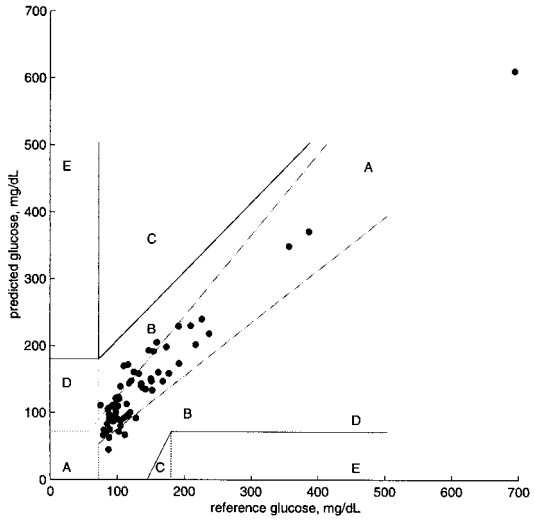

Fig. 5. Clarke error grid plot of glucose concentration predictions in serum. The predictions are all in the A and B regions, which are the desirable regions for clinical accuracy. See text for details.

uncertainty, which instead is limited by the error in the reference analyzer, even for the lowest integration time explored.

2. *Comparison of Observed RMSEP and Clinical Parameters*

This work is intended as a feasibility study and is not a measure of the ultimate accuracy that can be achieved by the Raman technique. Nevertheless, a short mention of some typical medical parameters is useful for placing the current results in a clinical context and for estimating the extent of necessary future improvements. Because glucose is of such importance to the community of diabetic patients, a special chart, called the Clarke error grid,[46] has been developed for plotting glucose predictions versus a reference technique. Simply reporting a percent error or an absolute error is not useful for a clinician facing a treatment decision. The grid method provides a qualitative sense of how useful or harmful the glucose predictions would be to a diabetic patient in various stages of hyper-glycemia or hypoglycemia; boundary lines are not to be regarded as absolute. Region A corresponds to a correct clinical decision based on the Raman-predicted value; region B, an acceptable clinical error in either direction; regions C through E, increasingly harmful incorrect decisions. For a method to be useful, most predictions should fall in the regions labeled A and B. Our serum glucose predictions are plotted on this chart in Fig. 5. In reporting the results of this initial study, we incorporate the error grid plot simply to provide a graphic sense that a RMSEP of 26 mg/dL begins to approach the level of clinical usefulness. The figure also reveals that none of our samples fell in the hypoglycemic region near 70 mg/dL, where prediction accuracy is most crucial; this was so because such samples were not readily available from our patient population. In a future study we hope to obtain or create samples that span this region. The inclusion of hypoglycemic samples should not present any fundamentally new challenges; as long as the basic assumptions of linear superposition are still met, the RMSEP for such samples will be the same as for any others.

Table 2. Comparison of Healthy Adult Ranges of Serum Analyte Concentrations[a] and RMSEP Values from PLS Concentration Predictions[b]

Analyte	Healthy Range	Δ_{conc}	RMSEP	Δ_{conc}/RMSEP
Glucose	70–110 mg/dL	40	26	1.5
Cholesterol	150–250 mg/dL	100	12	8.3
Triglyceride	10–190 mg/dL	180	29	6.2
BUN (urea)	8–23 mg/dL	15	3.8	3.9
Total protein	6.0–7.8 g/L	1.8	0.19	9.5
Albumin	3.2–4.5 g/L	1.3	0.12	10.8

[a]Ref. 47.
[b]The final column lists the ratio of the concentration range to the RMSEP, providing a roughly normalized index of the clinical relevance of the RMSEP. A higher ratio indicates finer resolution and therefore higher clinical relevance.

To provide clinical context for the other five analytes, we list in Table 2 the RMSEP values obtained for all six along with their associated concentration ranges for healthy adults.[47] The rightmost column provides a normalized index for the approximate number of resolvable concentration bins into which the RMSEP divides the healthy range. The larger this number, the more clinical resolution is provided by the RMSEP. As the table shows, the Raman predictions of albumin, total protein, and cholesterol have the highest values, from 8 to 11, and glucose, at 1.5, has the lowest clinical resolution. Although target accuracies depend on the particular application, this rough index correctly shows that the Raman glucose prediction accuracy would need to be improved to be clinically useful, whereas the Raman protein and lipid predictions in this study already achieve or closely approach clinically significant accuracy. Some specific threshold values for increases in analyte concentrations, taken from a 1978 survey of doctors' opinions on medical decision making,[48] are the following: BUN, 6 mg/dL (patient on daily dosage of gentamicin sulfate); cholesterol, 20 mg/dL (routine physical); and triglyceride, 20 mg/dL (routine physical). In the first two cases, the current Raman RMSEP is lower than the threshold value for clinical action; in the third case it is 50% higher.

3. *Calibration Checks*

As was mentioned above, a simple wave-number calibration, with a peak near 1000 cm^{-1} used as an internal standard, was performed; however, this calibration did not totally remove the effects of drift. Leave-half-out cross validations (weeks 1–4 and weeks 5–7 predicting each other) were performed to measure the robustness of the leave-one-week-out procedure against system drift. To correct for the effect of having smaller calibration sets than in the leave-one-week-out analysis, odd–even cross valida-

Table 3. Comparison of RMSEP Values for Odd–Even and Half-and-Half (i.e., Leave-Half-Out) Cross Validations[a]

Analyte	Odd–Even RMSEP	Half and Half RMSEP	Increase (%)
Glucose	24 mg/dL	30	25
Cholesterol	13 mg/dL	15	15
Triglyceride	29 mg/dL	32	10
BUN	3.3 mg/dL	3.5	6
Total protein	0.21 g/dL	0.21	0
Albumin	0.14 g/dL	0.15	7

[a]See text for details. 300-s spectra were used in both cases.

tions (the odd-numbered and even-numbered weeks predicting each other) were also performed; these too had smaller calibration sets but permitted overlap between the dates on which calibration and validation data were gathered. Results of these cross validations, performed with 300-s data to yield the best possible results, are listed in Table 3, with leave-half-out plots for three analytes (glucose, cholesterol, and albumin) shown in Fig. 6. As Table 3 reveals, the leave-half-out RMSEP values are higher than the corresponding odd–even values by factors that range from 0 to 25%, with only glucose higher than 15%. The calibrations therefore do have some instability against system drift, which should be studied further to correct more carefully for its effects. However, even with the modest amount of wave-number calibration performed in this study, the extent of the instability is relatively minor over the scale of seven weeks, especially for analytes other than glucose.

Although a prediction plot demonstrates the ability of PLS to extract concentration predictions, it is the line shapes from the calibration process, namely, the weight vectors and the overall *b*-vector, that illuminate the underlying physical correlation. Figure 7 compares the second glucose weight vector and the glucose *b*-vector with a spectrum of pure aqueous glucose that was acquired independently and binned over five pixels in the same way as the PLS-analyzed data. From all the weight vectors, the second was chosen because the glucose peaks are most evident there; there is no particular significance to its being

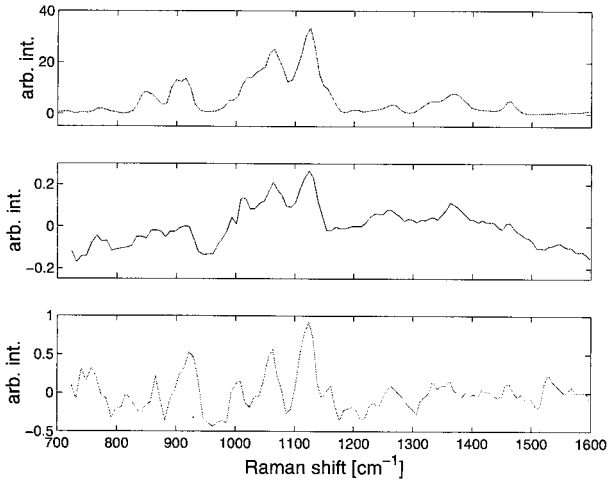

Fig. 7. Comparison of pure glucose Raman spectrum in saline (top), second PLS weight vector for glucose in serum (middle), and PLS *b*-vector for glucose prediction in serum (bottom). The appearance of glucose features in the weight vector and the *b*-vector demonstrate that the multivariate analysis has extracted the Raman signature of glucose.

the second one derived. The prominent spectral features in the weight vector and the *b*-vector have the same shape as the spectrum of glucose at those wave numbers, showing that the PLS predictions are indeed based on the Raman signature of glucose. Similar verifications for other analytes will performed in the future, as discussed below.

Another important check on the significance of PLS predictions is a table of the correlation coefficient $(\sigma_{ij}^2/\sigma_i\sigma_j)$ among different analytes' reference concentrations; this information is provided in Table 4. If two analytes in a training set have highly correlated concentrations, then PLS can predict both by using the signal from only one; if the correlation is not valid for the entire population from which the training set is drawn, then the accuracy of the cross-validation results can be spurious. From the table, however, we can see that the only large correlation, between albumin and total protein, is an expected one, because albumin is the main protein in serum.

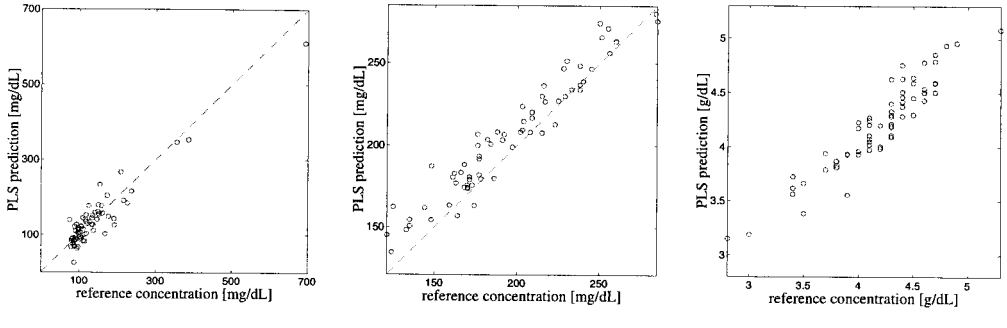

Fig. 6. PLS leave-half-out predictions of analyte concentrations in serum. The accuracy of the predictions implies that system drift effects are minor; see also Table 3 and the discussion in text. (a) Glucose, (b) cholesterol, (c) albumin.

Table 4. Correlation Coefficient Between Different Analytes' Concentrations in the Serum Analysis Study[a]

	G	C	Tr	B	Tp	A
G	1	−0.06	0.06	0.25	−0.09	−0.14
C		1	0.18	−0.09	0.11	0.19
Tr			1	0.01	−0.02	−0.03
B				1	−0.14	−0.17
Tp					1	0.62
A						1

[a]G, glucose; C, cholesterol; Tr, triglyceride; B, BUN; Tp, total protein; A, albumin. See text for details.

The remaining low correlation coefficients in Table 4 indicate that the calibrations for other analytes are based on separate spectral signatures and contain no spurious results.

Table 5. PLS Prediction Results for Whole Blood Data Set

Analyte	Reference Error	RMSEP	r^2	PLS Model Rank
Glucose	3 mg/dL	79 mg/dL	0.18	10
Cholesterol	4 mg/dL	40 mg/dL	0.19	12
Triglyceride	3 mg/dL	80 mg/dL	0.55	10
BUN (urea)	0.9 mg/dL	5.9 mg/dL	0.65	12
Total protein	0.1 g/dL	0.35 g/dL	0.62	9
Albumin	0.09 g/dL	0.27 g/dL	0.67	12

B. Whole Blood

The prediction parameters and RMSEP values for the same six analytes are given in Table 5 for the whole blood data set, and the corresponding prediction plots appear in Fig. 8. There were no obvious outliers in the data set; therefore spectra of all 69 samples were included in the analysis, with a fixed spectral range of 720–1602 cm^{-1}. For maximum prediction accuracy, the full 5 min of spectral data were needed. As anticipated, prediction accuracy decreased for all six analytes relative to the serum results. For glucose, in particular, the predictive result is not significant. However, four of the other analytes still exhibit significant correlation between the Raman-derived and reference concentrations. The additional analytical parameter, hematocrit, was predicted with high accuracy, as shown in Fig. 9. We obtained these predictions by processing the data as if blood were a clear medium, and as such the results are preliminary. We expect that a model incorporating the variable turbidity of blood should yield improved accuracy; attempts to develop such a model are under way.

Note that the SNR for signals measured in whole blood is lower than in serum, as evidenced in Fig. 10. The figure shows dissolved glucose spectra obtained in phosphate-buffered saline (same data as in the top panel of Fig. 7), serum, and whole blood, with a spec-

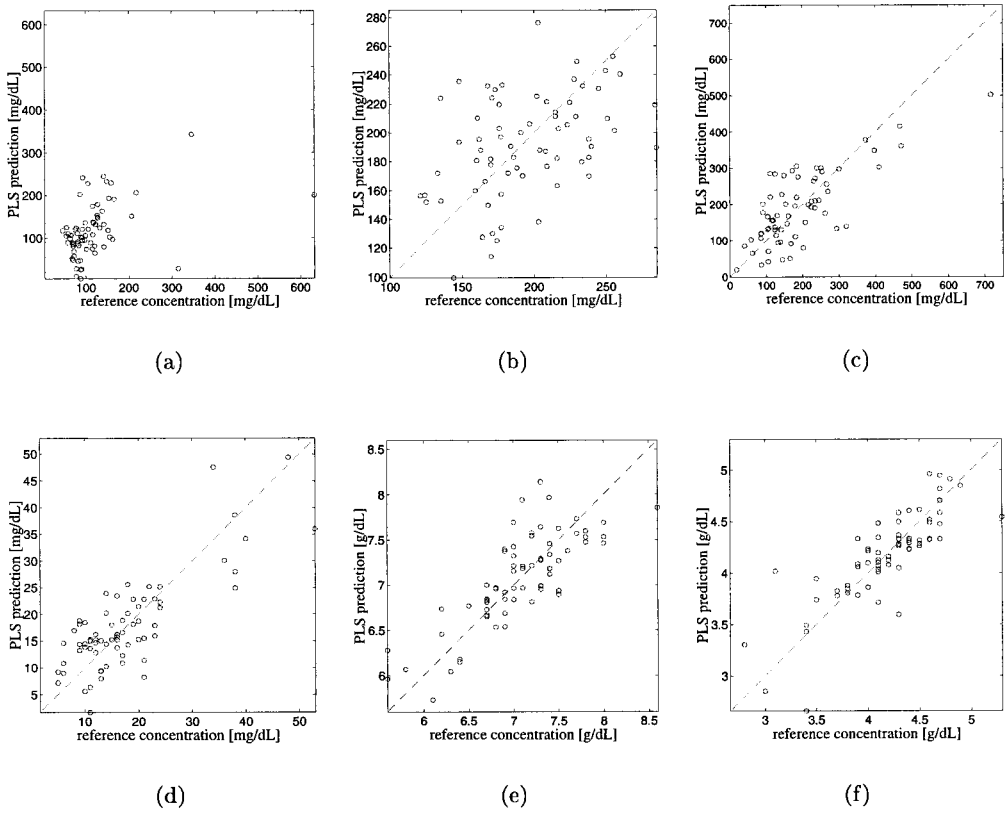

Fig. 8. PLS predictions of serum analyte concentrations from whole blood data. Although the plots are all less accurate than the results achieved for serum, four of the plots have visible correlations with r^2 values greater than 0.5. (a) Glucose, (b) cholesterol, (c) triglyceride, (d) urea (BUN), (e) total protein, (f) albumin.

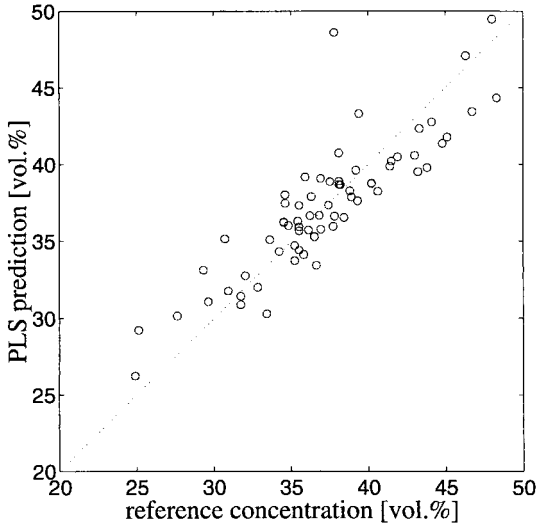

Fig. 9. Hematocrit cross-validation results for whole blood samples. The RMSEP is 2.7 percentage units, with an r^2 of 0.73. Reference analyzer accuracy is 0.4 percentage unit.

trum of the medium alone subtracted in all cases to remove the effects of the medium and the instrument. Although the saline and serum signals are nearly equal, the whole blood signal is approximately four times weaker. Coupled with the fact that the serum generates only approximately twice as much spectral background as whole blood, and therefore only 1.4 times as much shot noise, this means that the SNR in blood is smaller by a factor of ~3. This reduced SNR in the whole blood calibration set relative to the serum data set presumably also contributes to the observed decrease in prediction accuracy.

4. Conclusions

We have demonstrated that Raman spectra of serum and whole blood can be acquired and analyzed by use of PLS to extract concentration predictions of many important blood analytes. In serum, the results can be obtained rapidly (10–60 s) for six analytes. Examination of the PLS *b*-vector for glucose confirms a spectral correlation with the known Raman line shape of that analyte. Preliminary processing of whole blood data, with no correction for the effects of turbidity, nevertheless yields significant prediction accuracy for four of six analytes predicted in serum and additionally for hematocrit. Leave-one-week-out cross validations, supported by leave-half-out checks, demonstrate that the PLS calibrations are fairly robust against fluctuations in the alignment of the measuring system, although an increase in the glucose RMSEP suggests that further attempts to correct for drift are warranted. These results indicate the level of practicality and sensitivity of Raman spectroscopy for potential blood analysis applications.

Future research will address concentration calculations and the effects of turbidity. The concentration predictions here were generated with PLS and used the known Raman spectrum of glucose solely to validate the calibration (Fig. 10); however, we recently developed a new calibration technique that incorporates an analyte's spectrum directly into the calibration procedure. This technique, called hybrid linear analysis, has been shown to generate more-accurate calibrations than PLS.[49,50] For consistency, PLS was used for all results reported here, but once a more comprehensive set of pure analyte spectra is obtained (only glucose was measured as of this writing), the data will be reanalyzed by hybrid linear analysis. PLS weight vectors and *b*-vectors will also be compared with these pure analyte spectra, as mentioned above. In addition, a study is under way to aid in the understanding of the effects of whole blood turbidity on Raman signal strength, linearity, and spatial distribution in an attempt to improve both our signal collection and our concentration prediction technique.

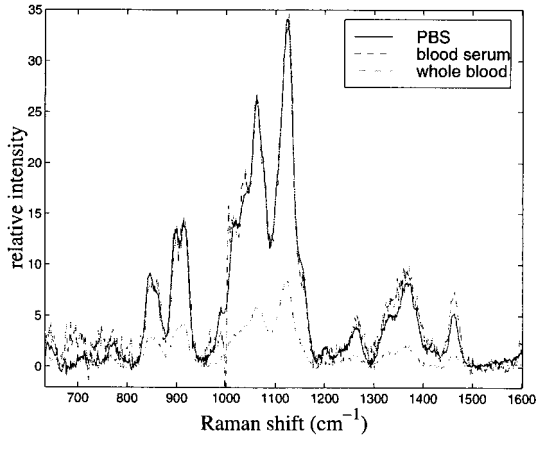

Fig. 10. Spectra of glucose obtained in saline (PBS), serum, and whole blood. The signal from blood is seen to be approximately four times lower than that from the nonturbid media.

The authors thank Susan Chin, Virginia Ching, Cynthia Provencher, Duc Khuc, and Neil O'Neill, technologists at Beth Israel Deaconess Medical Center, for obtaining the blood samples and performing the reference measurements. This research was conducted at the Laser Biomedical Research Center of the G. R. Harrison Spectroscopy Laboratory at MIT, with support from National Institutes of Health grant 5-P41-RR02594 and Chiron Diagnostics Corporation.

References

1. B. Bauer and T. Floyd, "Monitoring of glucose in biological fluids by Fourier-transform infrared spectrometry with a cylindrical internal reflectance cell," Anal. Chim. Acta **197,** 295–301 (1987).
2. Y. Mendelson, A. C. Clermont, R. A. Peura, and B.-C. Lin, "Blood glucose measurement by multiple attenuated total reflection and infrared absorption spectroscopy," IEEE Trans. Biomed. Eng. **37,** 458–465 (1990).
3. H. M. Heise, R. Marbach, T. Koschinsky, and F. A. Gries, "Multicomponent assay for blood substrates in human plasma

by mid-infrared spectroscopy and its evaluation for clinical analysis," Appl. Spectrosc. **48,** 85–95 (1994).
4. H. M. Heise and A. Bittner, "Investigation of experimental errors in the quantitative analysis of glucose in human blood plasma by ATR-IR spectroscopy," J. Mol. Struct. **348,** 21–24 (1995).
5. K. J. Ward, D. M. Haaland, M. R. Robinson, and R. P. Eaton, "Post-prandial blood glucose determination by quantitative mid-infrared spectroscopy," Appl. Spectrosc. **46,** 959–965 (1992).
6. R. Simhi, D. Bunimovich, B.-A. Sela, and A. Katzir, "Multicomponent analysis of human blood using fiberoptic evanescent wave spectroscopy," in *Medical Sensors II and Fiber Optic Sensors*, F. Baldini, P. R. Coulet, A. M. Verga Scheggi, and O. S. Wolfbeis, eds., Proc. SPIE **2331,** 166–172 (1994).
7. G. Budínová, J. Salva, and K. Volka, "Application of molecular spectroscopy in the mid-infrared region to the determination of glucose and cholesterol in whole blood and in blood serum," Appl. Spectrosc. **51,** 631–635 (1997).
8. M. A. Arnold and G. W. Small, "Determination of physiological levels of glucose in an aqueous matrix with digitally filtered Fourier transform near-infrared spectra," Anal. Chem. **62,** 1457–1464 (1990).
9. F. M. Ham, I. N. Kostanic, G. M. Cohen, and B. R. Gooch, "Determination of glucose concentrations in an aqueous matrix from NIR spectra using optimal time-domain filtering and partial least-squares regression," IEEE Trans. Biomed. Eng. **44,** 475–484 (1997).
10. G. Spanner and R. Niessner, "New concept for the non-invasive determination of physiological glucose concentration using modulated laser diodes," Fresenius J. Anal. Chem. **354,** 306–310 (1996).
11. D. M. Haaland, M. R. Robinson, G. W. Koepp, E. V. Thomas, and R. P. Eaton, "Reagentless near-infrared determination of glucose in whole blood using multivariate calibration," Appl. Spectrosc. **46,** 1575–1578 (1992).
12. E. Peuchant, C. Salles, and R. Jensen, "Determination of serum cholesterol by near-infrared reflectance spectrometry," Anal. Chem. **59,** 1816–1819 (1987).
13. J. W. Hall and A. Pollard, "Near-infrared spectrophotometry: a new dimension in clinical chemistry," Clin. Chem. **38,** 1623–1631 (1992).
14. A. Bittner, R. Marbach, and H. M. Heise, "Multivariate calibration for protein, cholesterol and triglycerides in human plasma using short-wave near-infrared spectrometry," J. Mol. Struct. **349,** 341–344 (1995).
15. R. Marbach, T. Koschinsky, F. A. Gries, and H. M. Heise, "Noninvasive blood glucose assay by near-infrared diffuse reflectance spectroscopy of the human inner lip," Appl. Spectrosc. **47,** 875–881 (1993).
16. M. R. Robinson, R. P. Eaton, D. M. Haaland, G. W. Koepp, E. V. Thomas, B. R. Stallard, and P. L. Robinson, "Noninvasive glucose monitoring in diabetic patients: a preliminary evaluation," Clin. Chem. **38,** 1618–1622 (1992).
17. K.-U. Jagemann, C. Fischbacher, K. Danzer, U. A. Müller, and B. Mertes, "Application of near-infrared spectroscopy for noninvasive determination of blood/tissue glucose using neural networks," Z. Phys. Chem. **191,** 179–190 (1995).
18. G. L. Coté, M. D. Fox, and R. B. Northrop, "Noninvasive optical polarimetric glucose sensing using a true phase measurement technique," IEEE Trans. Biomed. Eng. **39,** 752–756 (1992).
19. T. W. King, G. L. Coté, R. McNichols, and M. J. Goetz, "Multispectral polarimetric glucose detection using a single Pockels cell," Opt. Eng. **33,** 2746–2753 (1994).
20. B. D. Cameron and G. L. Coté, "Noninvasive glucose sensing utilizing a digital closed-loop polarimetric approach," IEEE Trans. Biomed. Eng. **44,** 1221–1227 (1997).
21. M. Kohl, M. Cope, M. Essenpreis, and D. Bocker, "Influence of glucose concentration on light scattering in tissue-simulating phantoms," Opt. Lett. **19,** 2170–2172 (1994).
22. J. S. Maier, S. A. Walker, S. Fantini, M. A. Franceschini, and E. Gratton, "Possible correlation between blood glucose concentration and the reduced scattering coefficient of tissues in the near infrared," Opt. Lett. **19,** 2062–2064 (1994).
23. J. R. Bruulsema, J. E. Hayward, T. J. Farrell, M. S. Patterson, L. Heinemann, M. Berger, T. Koschinsky, J. Sandahl-Christiansen, and H. Orskov, "Correlation between blood glucose concentration in diabetics and noninvasively measured tissue optical scattering coefficient," Opt. Lett. **22,** 190–192 (1997).
24. G. Spanner and R. Niessner, "Noninvasive determination of blood constituents using an array of modulated laser diodes and a photoacoustic sensor head," Fresenius J. Anal. Chem. **355,** 327–328 (1996).
25. S. Y. Wang, C. E. Hasty, P. A. Watson, J. P. Wicksted, R. D. Stith, and W. F. March, "Analysis of metabolites in aqueous solutions by using laser Raman spectroscopy," Appl. Opt. **32,** 925–929 (1993).
26. J. P. Wicksted, R. J. Erckens, M. Motamedi, and W. F. March, "Raman spectroscopy studies of metabolic concentrations in aqueous solutions and aqueous humor specimens," Appl. Spectrosc. **49,** 987–993 (1995).
27. M. J. Goetz Jr., G. L. Coté, R. Erckens, W. March, and M. Motamedi, "Application of a multivariate technique to Raman spectra for quantification of body chemicals," IEEE Trans. Biomed. Eng. **42,** 728–731 (1995).
28. R. J. Erckens, M. Motamedi, W. F. March, and J. P. Wicksted, "Raman spectroscopy for non-invasive characterization of ocular tissue: potential for detection of biological molecules," J. Raman Spectrosc. **28,** 293–299 (1997).
29. X. Dou, Y. Yamaguchi, H. Yamamoto, S. Doi, and Y. Ozaki, "A highly sensitive, compact Raman system without a spectrometer for quantitative analysis of biological samples," Vib. Spectrosc. **14,** 199–205 (1997).
30. X. Dou, Y. Yamaguchi, H. Yamamoto, S. Doi, and Y. Ozaki, "Quantitative analysis of metabolites in urine using a highly precise, compact near-infrared Raman spectrometer," Vib. Spectrosc. **13,** 83–89 (1996).
31. X. Dou, Y. Yamaguchi, H. Yamamoto, H. Uenoyama, and Y. Ozaki, "Biological applications of anti-Stokes Raman spectroscopy: quantitative analysis of glucose in plasma and serum by a highly sensitive multichannel Raman spectrometer," Appl. Spectrosc. **50,** 1301–1306 (1996).
32. R. V. Tarr and P. G. Steffes, "Non-invasive blood glucose measurement system and method using stimulated Raman spectroscopy," U.S. patent 5,243,983 (14 September 1993).
33. R. V. Tarr and P. G. Steffes, "The noninvasive measure of D-glucose in the ocular aqueous humor using stimulated Raman spectroscopy," IEEE/LEOS Newslett. **12**(2), 22–27 (1998).
34. A. J. Berger, Y. Wang, and M. S. Feld, "Rapid, noninvasive concentration measurements of aqueous biological analytes by near-infrared Raman spectroscopy," Appl. Opt. **35,** 209–212 (1996).
35. A. J. Berger, I. Itzkan, and M. S. Feld, "Feasibility of measuring blood glucose concentration by near-infrared Raman spectroscopy," Spectrochim. Acta **53,** 287–292 (1997).
36. R. J. Henry, *Clinical Chemistry: Principles and Techniques* (Harper and Row, New York, 1964), pp. 650–651.
37. W. T. Caraway, "Carbohydrates," in *Fundamentals of Clinical Chemistry*, N. W. Tietz, ed. (Saunders, Philadelphia, Pa., 1970), pp. 154–156.
38. D. M. Haaland and E. V. Thomas, "Partial least-squares methods for spectral analyses. 1. Relation to other quantitative calibration methods and the extraction of qualitative information," Anal. Chem. **60,** 1193–1202 (1988).

39. P. Geladi and B. R. Kowalski, "Partial least-squares regression: a tutorial," Anal. Chim. Acta **185,** 1–17 (1986).
40. E. Sanchez and B. R. Kowalski, "Tensorial calibration. 1. First-order calibration," J. Chemom. **2,** 247–263 (1988).
41. A. J. Berger and M. S. Feld, "Analytical method of calculating chemometric prediction error," Appl. Spectrosc. **51,** 725–732 (1997).
42. G. Small and M. Arnold, "Data handling issues for near-infrared glucose measurements," IEEE/LEOS Newsletter **12** (2), 16–17 (1998).
43. P. R. Carey, *Biochemical Applications of Raman and Resonance Raman Spectroscopies* (Academic, New York, 1982), pp. 71–79.
44. S. Krimm, "Raman spectra and the conformations of biological macromolecules," in *Biological Applications of Raman Spectroscopy*, T. G. Spiro, ed. (Wiley, New York, 1987), Vol. 1, pp. 1–46.
45. K. Faber and B. R. Kowalski, "Improved prediction error estimates for multivariate calibration by correcting for the measurement error in the reference values," Appl. Spectrosc. **51,** 660–665 (1997).
46. W. L. Clarke, D. Cox, L. A. Gonder-Frederick, W. Carter, and S. L. Pohl, "Evaluating clinical accuracy of systems for self-monitoring of blood glucose," Diabetes Care **10,** 622–628 (1987).
47. C. E. Speicher and J. W. Smith, Jr., *Choosing Effective Laboratory Tests* (Saunders, Philadelphia, Pa., 1983), pp. 357–365.
48. L. P. Skendzel, "How physicians use laboratory tests," in *Using the Clinical Laboratory in Medical Decision-Making*, G. D. Lundberg, ed. (American Society of Clinical Pathologists, Chicago, 1984), Chap. 30, pp. 243–250.
49. A. J. Berger, T.-W. Koo, I. Itzkan, and M. S. Feld, "An enhanced algorithm for linear multivariate calibration," Anal. Chem. **70,** 623–628 (1998).
50. J. J. Qu, O. L. Yau, S. M. Yau, D. Suria, and B. C. Wilson, "Measurements of therapeutic drugs and substances of abuse in human body fluids by near-IR laser Raman spectroscopy with new algorithms," in *Biomedical Diagnostic, Guidance, and Surgical-Assist Systems*, D. A. Benaron, R. D. Bucholz, S. T. Charles, W. S. Grundfest, M. W. Vannier, and T. Vo-Dinh, eds., Proc. SPIE **3595,** (to be published).